Multiple x-ray diffraction to determine transverse and longitudinal lattice deformation in shocked lithium fluoride

P. A. Rigg* and Y. M. Gupta
Institute for Shock Physics and Department of Physics, Washington State University, Pullman, Washington 99164-2816
(Received 16 August 2000; published 9 February 2001)

Experimental and analytic developments are described that utilize multiple x-ray diffraction to determine real-time, lattice deformation in directions parallel and perpendicular to shock-wave propagation in single crystals. Using a monochromatic x-ray source, two Bragg reflections were obtained simultaneously from LiF crystals shocked along the [111] and [100] directions. Symmetry permitted the transverse lattice deformation to be determined by measuring interplanar spacing longitudinally and in one other direction. We chose this to be a [110] direction in both cases because the intensity of the (220) reflection is high and because the transverse deformation component from this measurement is relatively large. Due to the complex geometry involved, an analytic model was required to calculate the (220) peak shift under the deformation conditions of interest. This model was used both to design experiments and to analyze the results. It was determined that shock compression below 4 GPa along the [111] orientation—which results in macroscopic elastic deformation—produced, as expected, no transverse lattice deformation. In contrast, shock compression along the [100] orientation—which results in macroscopic elastic-plastic deformation—produced equal interplanar spacing changes along the longitudinal and transverse directions. The analytic developments and the implications of our results are discussed.

DOI: 10.1103/PhysRevB.63.094112 PACS number(s): 62.50.+p, 61.10.−i, 62.20.Fe

I. INTRODUCTION

A good understanding of shock-wave-induced deformation and structural changes at the microscopic level in condensed materials is a long-standing need.[1] In recent years, time-resolved optical spectroscopy methods have been used successfully to examine and understand chemical reactions in shocked liquids[2–4] and symmetry and structural changes in shocked solids.[5–7] Efforts to incorporate x-ray diffraction measurements into shock compression experiments have been less successful, despite several attempts reported in the literature.[8–20] Hence a precise determination and understanding of lattice deformation in the shocked state has been difficult.

Recently, we reported experimental developments[21,22] designed to overcome limitations in previous studies and obtained quantitative x-ray diffraction data corresponding to elastic and elastic-plastic deformation in shocked LiF single crystals. The terms ''elastic'' and ''elastic-plastic'' refer to material response at the continuum level. LiF was chosen because of the considerable body of continuum measurements and analyses under shock loading[23–29] and because of the strongly anisotropic response observed due to the activation of different slip systems when shocked along different orientations.[25,27] Shock compression along the [111] axis shows an elastic response up to ~4 GPa.[27] In contrast, an elastic-plastic response is observed when shocked along [100] to the same longitudinal stress.[23,24] This anisotropic response permitted an examination of lattice compression for both elastic and elastic-plastic deformations when the same material was subjected to comparable longitudinal stresses. X-ray diffraction was used to monitor interplanar spacing changes along the shock propagation direction. These results in conjunction with the Hugoniot data[30] showed that for elastic deformation, the unit cell is compressed uniaxially. However, elastic-plastic deformation resulted in isotropic unit-cell compression. Macroscopic volume compression in all cases is uniaxial.

These experiments[21] established the use of x-ray diffraction to quantitatively probe shock-induced deformation at the microscopic level. However, lattice deformation measurements were limited to the shock propagation direction. Thus continuum results and certain assumptions were needed to analyze the data. A more general examination and better understanding of lattice compression in shocked single crystals require measurements perpendicular and parallel to the shock propagation direction. For such measurements, the interplanar spacing of multiple sets of planes must be monitored during shock compression. Furthermore, it is desirable to obtain this information in a single experiment.

Generally, energy dispersive techniques such as Laue back reflection and transmission photography are used to obtain data simultaneously from many different planes. However, these methods are not compatible with shock-wave experiments due to the long exposure times and the diffracting geometry required. Currently, experimental constraints limit us to using monochromatic x rays. Most techniques using monochromatic x rays require that the crystal be rotated to obtain diffraction from more than one set of planes and, therefore, cannot be used in our work. However, one technique known as multibeam x-ray diffraction (or, simply, multiple diffraction) permits diffraction from two or more sets of diffraction planes simultaneously using a collimated, monochromatic x-ray source.

Here we describe experimental and analytic developments that permit real-time, multiple-diffraction measurements and analysis in plate impact experiments. These developments were used to determine unit-cell compression in shocked LiF single crystals. Diffraction data were obtained simulta-

neously from planes parallel to the shock front and from one other set of planes for shock propagation along the [111] and [100] directions. When LiF is shocked along the [100] direction, two measurements are sufficient to determine the unit-cell dimensions because of crystal symmetry (fcc) and the plane-wave loading condition. When shocked along the [111] direction below the elastic limit, unit-cell compression is expected to be uniaxial with no changes in the transverse direction. Measurement from only one other set of planes is required to confirm this.

Two previous attempts[19,20] to determine transverse lattice deformation in shock-compressed single crystals have been reported and these are reviewed in Sec. II. Section III describes the theoretical developments to obtain and interpret multiple-diffraction data from a shocked crystal. The experimental methods and results are presented in Secs. IV and V, respectively. The principal findings are summarized in Sec. VI.

II. REVIEW OF PREVIOUS WORK

Whitlock and Wark attempted to measure transverse lattice deformation in radiation-hardened LiF shock compressed along [100] by diffracting simultaneously from planes perpendicular and parallel to the shock propagation direction.[19] Shock waves were generated by laser ablation of a thin Al coating on the diffracting surface of the crystal. It was stated that, for the laser intensities used, the method produced peak longitudinal stresses of approximately 6 GPa in the samples. Half of the sample was shadowed from the driver beam to produce both a shocked and unshocked region during the experiment. Here 250-ps x rays—generated by laser ionization of Ti—were turned on 1 ns after the peak of the pressure drive pulse. Thus the shock wave had traveled less than 7 μm into the material at the time of x-ray exposure. Diffraction data from the (200) planes showed the ambient diffraction lines along with a broad signal at higher angles corresponding to diffraction from the $\sim$7-μm compressed portion of the 80-μm-thick crystal. Maximum compression was attributed to the largest angle in the broad signal above the background. The reported $\Delta d/d_0$ values for the three successful experiments performed were -5.0%, -5.2%, and -5.1%. These were stated to be consistent with the drive pressure at the time of x-ray exposure and the LiF Hugoniot.[30]

The x-ray diffraction profiles obtained from the (002) planes, designed to examine transverse compression, showed qualitatively similar signatures from the unshocked and shocked regions. Only a low-intensity tail toward higher angles (presumably the shock signature) and a slight difference in intensity distinguish the two signals. Again, the maximum compression corresponded to the largest angle in the shocked signature above the ambient background signal. The $\Delta d/d_0$ values for the (002) planes were inferred to be -6.6%, -7.8%, and -10.0% for the three experiments. The authors state these to be comparable to the axial strains expected at the temporal peak of the pressure pulse. However, these values are significantly larger than the values obtained from the longitudinal measurements, suggesting that compression is greater in the transverse direction. The authors claim that the larger transverse values indicate that relaxation occurs more rapidly in the longitudinal direction. This inference is difficult to understand. Our analysis of the data, discussed below, does not support their claim.

The reported values for the longitudinal and transverse strain lead to unit cell dimensions of 3.82 and 3.69 Å, respectively, compared to an initial value in both directions of 4.028 Å. The resulting volume compression in the peak state is $\mu = V_0/V - 1 = 0.256$. According to the LiF Hugoniot data,[30] this value corresponds to a longitudinal peak stress of 25 GPa in contrast to the authors' assumed stress of 6 GPa. This large discrepancy is either due to a gross miscalculation of the peak stress in their samples or to an incorrect interpretation of the (002) data. Several arguments suggesting the latter are given below.

A transmission measurement requires that the diffracted x rays pass through the entire thickness of the sample. For x rays of wavelength 2.63 Å passing through LiF at the Bragg angle, the photoelectric absorption depth is on the order of 20 μm. Because the peak of the pressure pulse had traveled only 7 μm into the 80-μm-thick sample at the time of the x-ray exposure, diffracted x rays from the shocked region would be attenuated by over 95% in passing through the remaining thickness of the sample. Hence detection of a shocked signature is very difficult at best. Detection of the shocked signature is further complicated by the fact that the probed region consisted of approximately 73 μm of ambient material and about 7 μm of compressed material that was subjected to a strain gradient. Given these factors, it is not surprising that a good diffraction signal was not observed from the shocked region in the transmission measurements; the data were likely incorrectly analyzed. We believe that a different approach is necessary to determine transverse lattice deformation. In contrast, the shocked signature from the (200) planes (Bragg reflection) should account for at least half of the observed intensity since the shocked region is the first 7 μm of the diffracting layer.

It is interesting to note that if the transverse lattice deformation is assumed zero, a more likely inference from their transmission measurement, the unit-cell compression would be one-dimensional. This inference would give a volume compression of $\mu = 0.054$. Assuming an elastic Hugoniot for LiF (based on the elastic constants[31]), this value corresponds to a peak stress of 7.3 GPa, closer to the 6 GPa reported peak stress. In radiation-hardened LiF shocked along [100], an initial elastic response is in good agreement with continuum measurements reported by Asay *et al.*[23] The possible conclusion of no transverse lattice deformation would be consistent with existing continuum data.

Zaretsky took a different approach[20] in an attempt to measure the transverse lattice deformation in a shock-wave experiment. He recognized that it was not necessary to measure the interplanar spacing change perpendicular to the shock front to determine the transverse lattice deformation. If the longitudinal lattice deformation is known,[21,22,32] a second measurement that contains a component of both the transverse and longitudinal deformations can provide the needed data. Zaretsky presented calculations describing the condi-

tions necessary to simultaneously obtain diffraction from planes perpendicular to the shock propagation direction and an arbitrary second set of diffraction planes using a single, monochromatic x-ray source. The calculations also related the diffraction peak shift from the second set of planes to the transverse lattice deformation.

In the experimental work, NaCl single crystals—backed by graphite windows—were shock compressed along the [100] axis using a 25-mm gas gun. Using a flash x-ray source, the (200) and (220) diffraction peaks were recorded simultaneously on a single detector. The (220) peak was a natural choice for the second diffraction peak because of its high intensity and because transmission of the diffraction signal through the crystal thickness is not necessary. Therefore, diffraction data for both peaks originate from the same probe depth in the crystal. Because of the spatial separation of the two peaks, a large detector is required to simultaneously record both peaks. A large-area charge-coupled device (CCD), if available, is cost prohibitive, and film does not provide the desired spatial resolution. Zaretsky's solution was to use a 75-mm scintillating screen to detect the x rays and reduce the output—using a fiber optic cone—to a 12.5-mm image for CCD detection. The experimental results were interpreted to infer one-dimensional compression of the unit cell in NaCl single crystals shocked well above the Hugoniot elastic limit (HEL). However, there are several problems with the experimental measurements and related analysis that make these results questionable. The inference of one-dimensional lattice compression above the HEL in a soft crystal is difficult to reconcile with our results.[21]

Zaretsky's calculations predicted that the transverse deformation is determined by the vertical shift of the (220) diffraction peak. As shown in Sec. V, these diffraction peaks are very tall in the vertical direction. Therefore, the combination of 6:1 imaging and a vertical shift that is small compared to the peak width may have precluded the detection of the vertical shift. Second, Zaretsky's analytical approach did not correctly account for the diffracting geometry involved in this problem, which is quite complicated in a multiple diffraction experiment. This issue will be discussed in more detail in the next section.

Zaretsky's approach had two major advantages: the complications associated with a transmission measurement[19] are avoided by employing a multiple-reflection technique, and the use of a plate impact facility produces uniform, planar loading. For these reasons, Zaretsky's approach could potentially be used to determine transverse lattice deformation in shock-compressed single crystals, but would require a more rigorous analytic and experimental development.

In summary, the past attempts to obtain transverse lattice deformation under shock loading are questionable.

III. THEORETICAL DEVELOPMENTS

Use of a collimated monochromatic source to obtain x-ray diffraction from multiple sets of diffracting planes in a single-crystal requires proper orientation of the crystal.[33] In general, when diffraction from only two sets of planes is desired, the Bragg condition is first satisfied for one set of

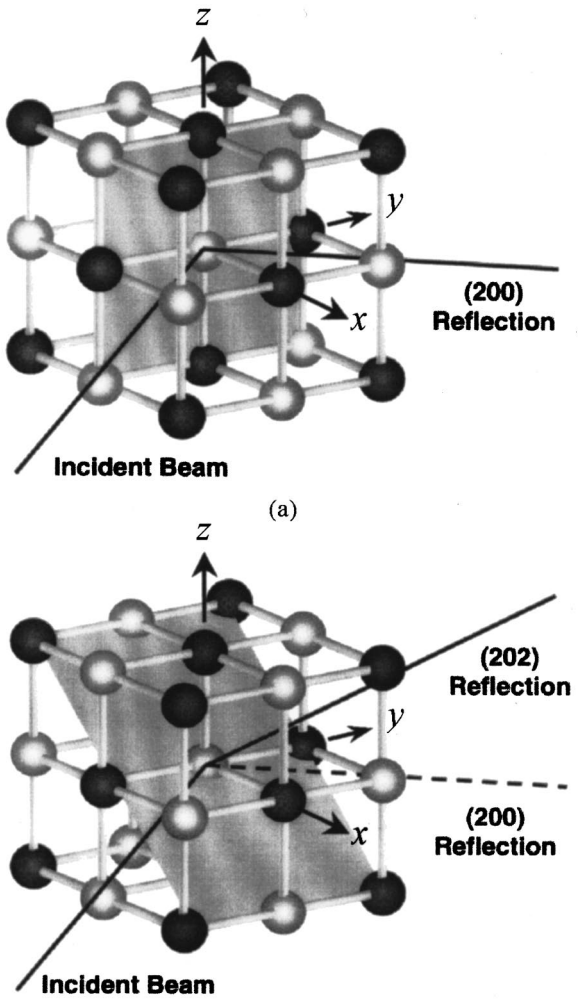

FIG. 1. Example of multiple diffraction from a single crystal using a monochromatic, collimated incident beam. The incident angle of the x rays is such that the Bragg condition is satisfied for the (a) (200) planes and (b) (202) planes, simultaneously.

planes. This is illustrated in Fig. 1(a) for diffraction from the (200) planes in the rocksalt structure. This Bragg condition holds for any arbitrary rotation of the crystal about the normal to those planes. However, for some particular rotations, the Bragg condition will be satisfied simultaneously for a second set of diffraction planes, as illustrated in Fig. 1(b). Usually, the first set of desired diffraction planes is parallel to the crystal surface and is referred to as the primary diffraction planes; the second set is referred to as the secondary diffraction planes.[33] In the calculations and experiments described here, the primary diffraction planes were always parallel to the shock front.

Because the normal to the primary planes is coincident with the normal to the crystal surface and both are coincident with the shock propagation direction, planar geometry is sufficient to relate the peak shift to the change in the Bragg angle due to lattice compression.[21,22,32] When the diffracting planes are not parallel to the shock front or the crystal surface, as is the case for the secondary planes, three-dimensional (3D) geometry arguments are required to relate the peak shift to changes in lattice compression. The effects

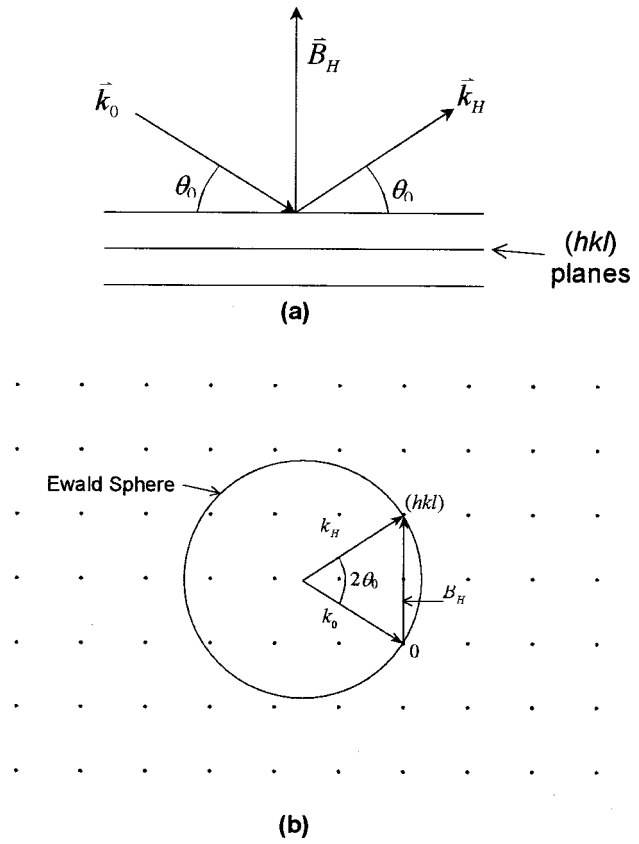

FIG. 2. X-ray geometry for diffraction from a single set of lattice planes as represented in (a) real space and (b) reciprocal space.

of a small divergence in the incident beam on both the shape and position of the diffraction peaks must also be considered explicitly. Additionally, effects of impact tilt on the position of the secondary reflection must be accounted for; these effects can be eliminated by the proper placement of the detector[21,32] for the primary reflection.

The experimental setup and data analysis required the development of an analytic model based on Bragg's law and the diffracting geometry of an arbitrary (hkl) reflection to predict (1) the configuration necessary to obtain multiple peaks in our plate impact facility, (2) the peak shape due to the divergence of the incident beam, (3) the effects of tilt and translation of the sample on the peak position, and (4) the peak shift expected for given loading and lattice deformation conditions. The model is described with respect to a laboratory reference frame defined such that the x axis is along the direction of shock propagation and the z axis is the vertical direction.

A. Reciprocal-space representation

Many x-ray diffraction problems are viewed optimally in reciprocal space using the Ewald construction.[34] This approach is particularly useful for discussing multiple diffraction. Figure 2 shows the x-ray geometry for diffracting from a single set of lattice planes in (a) real space and (b) reciprocal space. In reciprocal space, the crystal is represented by its reciprocal lattice and each lattice point represents one set of (hkl) lattice planes in the crystal. Figure 2(b) also shows the projection of the Ewald sphere, or sphere of reflection, used to visualize diffraction in reciprocal space. For a monochromatic, collimated incident x-ray beam, the sphere radius is $1/\lambda$, where λ is the x-ray wavelength. The wave vector $\mathbf{k}_0$, representing the incident x-ray beam, has a magnitude of $1/\lambda$, originates at the center of the Ewald sphere, and terminates at the origin of reciprocal space. For a set of (hkl) planes, the reciprocal lattice vector $\mathbf{B}_H$ points from the origin to the (hkl) reciprocal lattice point and has a magnitude of $1/d_H$, where d_H is the (hkl) interplanar spacing.

X-ray diffraction occurs when the Laue equation (equivalent to Bragg's law)

$$\mathbf{k}_H - \mathbf{k}_0 = \mathbf{B}_H \tag{1}$$

is satisfied, where $\mathbf{k}_H$ is the diffracted wave vector. Hence the (hkl) reciprocal lattice point lies on the surface of the Ewald sphere. Multiple diffraction occurs when two or more reciprocal lattice points lie simultaneously on the Ewald sphere. If the reciprocal lattice point in Fig. 2(b) corresponds to the primary diffraction planes, then a second point can be brought to the surface of the Ewald sphere by rotating the reciprocal lattice about $\mathbf{B}_H$. Because $\mathbf{B}_H$ is normal to the primary diffraction planes, this is equivalent to rotating the real lattice about this normal until the second diffraction peak is obtained.

B. Real-space representation

Reciprocal space and the Ewald sphere are convenient constructs for visualizing x-ray diffraction problems. However, the experimental setup and analysis require calculations of shock-induced diffraction peak position changes in real space. Throughout this section, we will take advantage of the fact that reciprocal-space vector directions are the same in real space (see Fig. 2).

To simulate the diffracted peak under ambient conditions, Eq. (1) is first used to determine all incident wave vectors in the divergent incident beam that will diffract from the crystal. This equation is then applied to each diffracting ray in the incident beam to find the corresponding diffracted wave vector. Knowledge of the incident and diffracted wave vectors makes it possible to use a ray tracing method to determine the location of the diffracted x rays on the detector.

Shock compression changes the crystal lattice in three fundamental ways: lattice compression, lattice tilt due to small deviations from planar impact, and lattice translation along the shock propagation direction. Lattice compression can change both the magnitude and direction of the reciprocal lattice vector $\mathbf{B}_H$. Changes to $\mathbf{B}_H$ in the shocked state are determined from the strain matrix corresponding to the loading conditions of interest. In this case, the strain matrix in the laboratory frame is given by[35]

$$E = \begin{pmatrix} \varepsilon_x & 0 & 0 \\ 0 & \varepsilon_y & 0 \\ 0 & 0 & \varepsilon_z \end{pmatrix}, \tag{2}$$

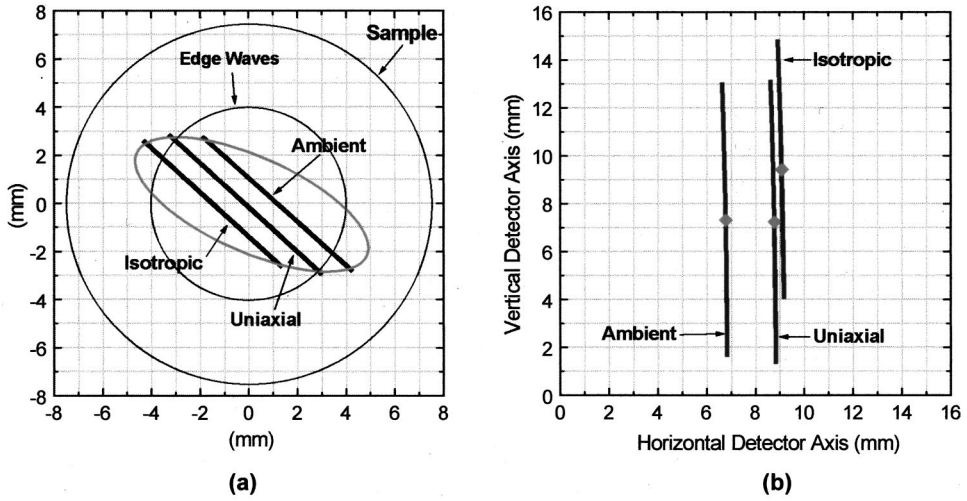

FIG. 3. Simulation of diffraction from the (202) planes in a [100]-oriented crystal under both ambient and shocked conditions showing (a) where diffraction occurs on the sample and (b) the expected diffraction peaks on the detector. Note that both uniaxial and isotropic compression are considered in the simulation.

where ε_x, ε_y, and ε_z are the strains in the *x*, *y*, and *z* directions, respectively.

To determine strain-induced changes in the reciprocal lattice vector, we write $\mathbf{B}_H$ as

$$\mathbf{B}_H = hb_x\hat{x} + kb_y\hat{y} + lb_z\hat{z}, \tag{3}$$

where b_x, b_y, and b_z are the inverse dimensions of an orthorhombic unit cell with sides parallel to the reference frame axes $(\hat{x},\hat{y},\hat{z})$. If the reference axes coincide with the crystallographic axes, then b_x, b_y, and b_z are simply the inverse of the conventional unit-cell dimensions: a_x, a_y, and a_z. For a unit cell subjected to a strain defined by Eq. (2), the cell dimensions will change by $\varepsilon_x a_x$, $\varepsilon_y a_y$, and, $\varepsilon_z a_z$, respectively. Thus the deformed unit cell will have an *x* dimension of

$$a_x' = (1-\varepsilon_x)a_x \tag{4}$$

and the *x* component of the reciprocal lattice vector will be

$$b_x' = \frac{1}{a_x'} = \frac{1}{(1-\varepsilon_x)a_x} = \frac{b_x}{(1-\varepsilon_x)}. \tag{5}$$

With similar expressions for the *y* and *z* components, the reciprocal lattice vector becomes

$$\mathbf{B}_H' = \frac{hb_x}{(1-\varepsilon_x)}\hat{x} + \frac{kb_y}{(1-\varepsilon_y)}\hat{y} + \frac{lb_z}{(1-\varepsilon_z)}\hat{z}. \tag{6}$$

For shock-wave propagation along directions other than [100], the values of b_x, b_y, and b_z must be determined through a coordinate transformation.

Impact tilt, measured in each experiment, changes the direction of both the reciprocal lattice vector and the normal to the crystal surface. For the purposes of this calculation, tilt can be interpreted as a rotation operator that operates on the two vectors. Lattice translation—due to shock-wave-induced motion—is in the *x* direction only and changes the spatial position of the crystal surface. The resulting horizontal shift in peak position is easily compensated for in the analysis from the amount of translation determined from the particle velocity in the experiment. Applying Bragg's law to the compressed, tilted, and translated lattice gives the new peak position due to shock compression. We can then compare this position to the ambient peak position to determine the expected peak shift for specific loading and deformation conditions.

Although the diffraction peak shift calculations can be performed for many different (hkl) planes, accurate determination of the transverse lattice deformation requires that the secondary diffraction planes satisfy the following conditions: (1) have diffraction peaks with sufficient intensity to be detected and (2) compression of these planes should produce a sufficiently large component perpendicular to the shock propagation direction to permit a quantitative determination of the transverse lattice deformation. For LiF single crystals shocked along the [111] and [100] directions, the {220} planes meet these criteria. Specifically, the (220) reflection is monitored for shock propagation along [111], while the (202) reflection [equivalent to (220) in a cubic crystal] is monitored for shock propagation along the [100] direction.

C. Simulation of the diffraction peak shifts

Figure 3 shows the results from a representative calculation for diffraction from the (202) planes in LiF shocked to a final stress of 2.5 GPa along the [100] direction. Both uniaxial and isotropic compression of the unit cell, for a given macroscopic longitudinal lattice deformation, were considered for this calculation. Calculations corresponding to diffraction from the (220) planes in a crystal shocked along [111] are qualitatively similar[32] to those presented in Fig. 3. In Fig. 3(a), the large circle represents the sample while the smaller circle indicates the approximate location of edge release at the time of the x-ray measurement. The ellipse shown represents the projection of the diverging incident x-ray cone on the sample surface, while the lines within the ellipse represent the points of incidence of the diffracting x rays on the crystal surface. The horizontal and vertical axes in Fig. 3(a) represent the horizontal and vertical laboratory frame axes $\hat{y}^L$ and $\hat{z}^L$. The ellipse and lines within the ellipse are tilted with respect to the laboratory frame as a result of the position of the x-ray source (see Fig. 5).

Figure 3(b) represents the plane of the CCD detector, and here the axes represent the horizontal and vertical axes of the detector itself. The lines shown in Fig. 3(b) represent the diffraction peaks from ambient and shock-compressed states of the crystal. The vertical height of the peak is a direct consequence of the divergence of the incident beam. As shown in Fig. 3(a), the Bragg condition is satisfied for a set of incident x rays spanning the divergence of the beam. Reducing the divergence of the incident beam reduces the height of the diffraction peak, but also reduces the intensity and the ability to satisfy the Bragg condition under a variety of shock loading conditions. Therefore, a balance has to be determined between these competing requirements.

The diffraction peaks resulting from both uniaxial and isotropic compression are generated using the strain matrix. The value of ε_x is determined directly from the diffraction measurement for the primary planes and serves as an input parameter for the calculation. For uniaxial compression, we assume that $\varepsilon_y = \varepsilon_z = 0$ at the lattice level, while for isotropic compression we assume that $\varepsilon_y = \varepsilon_z = \varepsilon_x$ at the lattice level. The diffraction peak shift is then calculated as the distance between the vertical centers of the ambient and shocked peaks. Qualitatively, uniaxial compression is characterized by mostly a horizontal shifting of the diffraction peak, as shown in Fig. 3(b), whereas the shift due to isotropic compression exhibits both a significant horizontal and a vertical component.

The fundamental differences in the vertical peak shifts for the uniaxial and isotropic lattice compression can be understood by considering the corresponding crystal symmetry changes due to shock compression and Bragg's law. Consider the conventional unit cell of LiF oriented such that the crystallographic axes coincide with the laboratory frame axes and the [100] axis points in the x direction (see Fig. 1). In this case, the reciprocal lattice vector of the (202) planes lies in the x-z plane at 45° from the x axis. Next, consider a plane that contains both the reciprocal lattice vector and the y (or [010]) axis, and let it also contain the incident wave vector $\mathbf{k}_i$. Then, by Bragg's law, the diffracted wave vector $\mathbf{k}_H$ must also lie in that plane. Under isotropic compression, crystal symmetry does not change; a cubic unit cell remains cubic, but with a reduced lattice parameter a'. If it is assumed that the orientation of the unit cell also remains unchanged, then the plane containing $\mathbf{k}_i$, $\mathbf{B}_H$, and $\mathbf{k}_H$ will be the same under both ambient and shocked conditions. The corresponding shift of the diffraction peak must also be in this plane, and since this plane is inclined at 45° with respect to the horizontal plane, the peak shift will have both a horizontal and vertical component, as seen on the detector.

The uniaxial case is quite different. Under uniaxial compression along the [100] direction, the unit cell goes from cubic to tetragonal symmetry. This changes the angle of $\mathbf{B}_H$ with respect to the x axis to less than 45°, which necessarily changes the inclination angle of the plane containing $\mathbf{k}_i$ and $\mathbf{k}_H$ by the same amount. This change in the inclination angle effectively keeps the diffraction peak shift roughly horizontal and explains the marked difference [Fig. 3(b)] between the two cases. Arguments for compression along the [111] direction are somewhat similar, but more difficult to visualize. In that case, uniaxial compression changes the crystal symmetry from cubic to rhombohedral, but still moves the reciprocal lattice vector of the secondary planes closer to the horizontal plane.

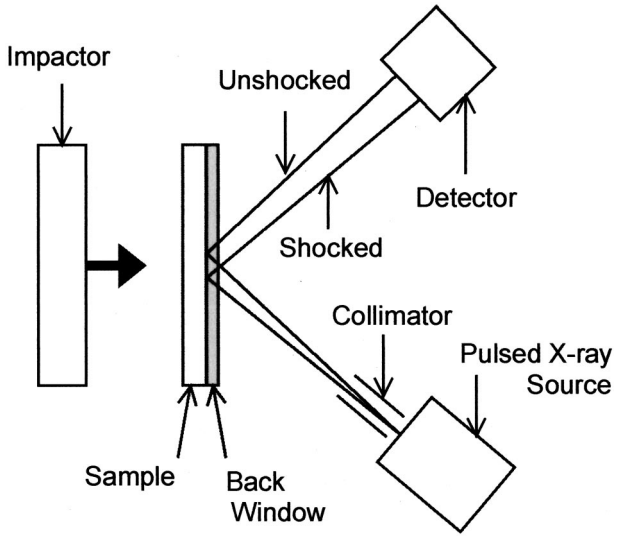

FIG. 4. Schematic view of the experimental configuration used to obtain real-time x-ray diffraction measurements from shock-compressed single crystals.

Although the vertical shifts are quite different between the uniaxial and isotropic cases, the horizontal shifts are very similar, illustrating the importance of accurately determining the vertical peak shift component in these measurements. However, the height of the peak in the vertical direction makes this determination inherently difficult.

IV. EXPERIMENTAL METHOD

The experimental configuration for obtaining x-ray diffraction data from a single set of planes in a shocked single crystal is shown schematically in Fig. 4. Because details regarding single-diffraction experiments have been presented elsewhere,[22] only brief comments are presented here. An intense 50-ns burst of $K\alpha$ x rays was produced from a 300-kV flash x-ray tube (Hewlett-Packard) with copper as the anode material ($\lambda = 1.54$ Å). A pinhole collimator (800-μm aperture) was used to enhance spatial resolution while permitting the needed divergence (20–25 mrad for the experiments described here) in the incident beam to obtain diffraction data from the shocked state. Furthermore, the use of a pinhole collimator produced a Gaussian-like vertical peak profile, making identification of the vertical peak center possible. The diffracted signal was incident upon a phosphor screen coupled to a two-dimensional detector array (EG&G 1254 Intensified Vidicon or Princeton Instruments CCD) to record the intensity vs diffraction angle data. The x-ray source and detector were arranged to satisfy the Bragg condition

$$\lambda = 2d \sin\theta, \tag{7}$$

for crystal planes perpendicular to the shock propagation direction. Here λ is the wavelength of incident x rays, d is the interplanar spacing, and θ is the diffraction angle.

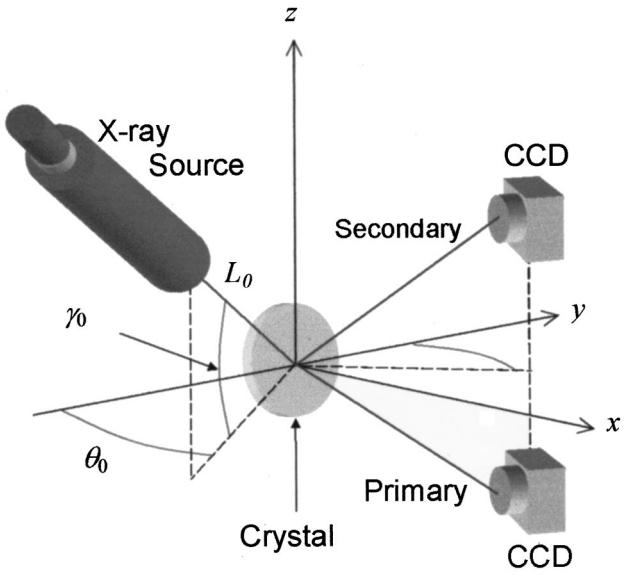

FIG. 5. Experimental configuration used for multiple x-ray diffraction measurements in shock-compressed LiF during a plate impact experiment. Adjustment of the x-ray source is allowed in both the horizontal and vertical planes to bypass constraints imposed by our plate impact facility, and separate CCD's are used to detect each diffraction peak. The *x* axis indicates the direction of shock propagation in the sample.

To obtain diffraction from planes parallel to the shock front or the primary diffraction planes [(111) or (200) planes] and the (220) planes simultaneously is, in principle, straightforward as described in the previous section. However, detecting this second peak is not straightforward in practice. To obtain the second diffraction peak, the crystal orientation about the normal to the primary planes must be within $\pm 1°$ of the optimal orientation. Hence careful orientation of the specimen using back reflection Laue photography is required prior to the experimental setup. The arrangement in Fig. 4 makes it difficult to detect the second peak outside the target chamber area due to the restrictive size of the chamber.[22] Even if this can be done, the spatial separation of the two peaks will be too large in most cases to detect on a single, average-sized detector (26 mm$\times$28 mm for CCD's used here) without sacrificing spatial resolution. These difficulties were overcome by using the experimental configuration shown in Fig. 5. In contrast to our previous method,[21,22] a second degree of freedom was added to the motion of the x-ray source to permit adjustment of the incident angle in both the horizontal and vertical planes. This change allowed greater flexibility in setting up the system for multiple-diffraction experiments.

Single crystals of ultrapure, optical-grade LiF (Bicron) were oriented to obtain simultaneous diffraction from the two sets of planes, and a Princeton Instruments CCD was used to detect each peak separately. The x-ray source and pinhole collimator, shown in Fig. 4, were again used. In addition to enhancing spatial resolution and permitting the needed divergence to obtain diffraction data from the shocked state, the collimator also gives the diffraction peak a Gaussian-like vertical profile, which permits determination

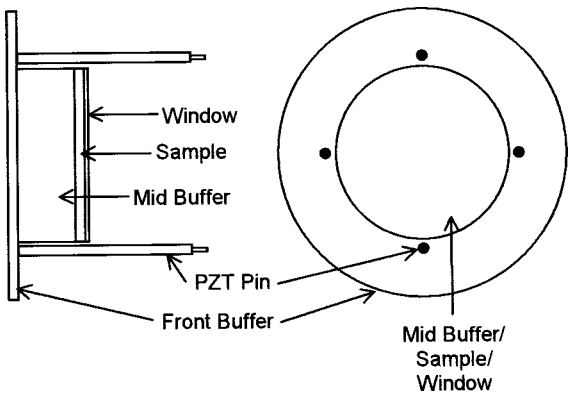

FIG. 6. The target assembly showing typical material locations and thicknesses, and the concentric arrangement of piezoelectric trigger pins around the sample.

of the vertical peak center. In all experiments, ambient diffraction peaks—used as reference—were obtained just prior to shocking the crystal.

Shock waves were generated by impacting 6061-T6 aluminum flyer plates, accelerated in a powder gun to desired velocities,[22] onto the sample assembly shown in Fig. 6. This assembly consisted of two buffer layers, both z-cut α-quartz (Valpey Fisher); the single-crystal LiF sample; and a vitreous carbon (Alfa Aesar) back window. Four piezoelectric pins (Dynasen, Inc.) were placed concentrically around the sample behind the front buffer to provide a trigger for the x-ray system and recording equipment, and to measure the impact tilt.[22,32] The midbuffer was used to delay the arrival of the shock wave at the probed region of the crystal to offset the insertion delay of the x-ray system. The back window was used to extend the duration of the shocked state in the probed region to improve synchronization of the x-ray pulse with the shock-wave event.

Figure 7 shows a snapshot of the calculated stress profile in the target at the time of peak x-ray exposure along with the x-ray probe depth in the LiF sample. Upon arrival of the shock wave at the LiF/vitreous carbon interface, the input stress drops due to the impedance mismatch between the two materials. This stress drop propagates back into the LiF sample as shown in the figure. The final stress—referred to as the reflected stress—is then maintained at the crystal/window interface until release waves from the back of the window arrive at the interface. The time at which this occurs depends on the wave speed and thickness of the window material. Because the window absorbs x rays, its thickness must be kept to a minimum. A 0.25-mm-thick vitreous carbon window reduced the diffracted x-ray intensity by 60%, but extended the duration of the shocked state in the probed region to approximately 100 ns. However, the timing jitter in our experiments reduced the usable time duration to about 50 ns. Since the x-ray pulse duration is 50–90 ns, synchronization requires considerable care. Further discussion of the experimental techniques can be seen elsewhere.[22,32]

V. EXPERIMENTAL RESULTS AND DISCUSSION

Nine experiments were performed in this study. Five were on LiF shocked along the [111] direction below the elastic

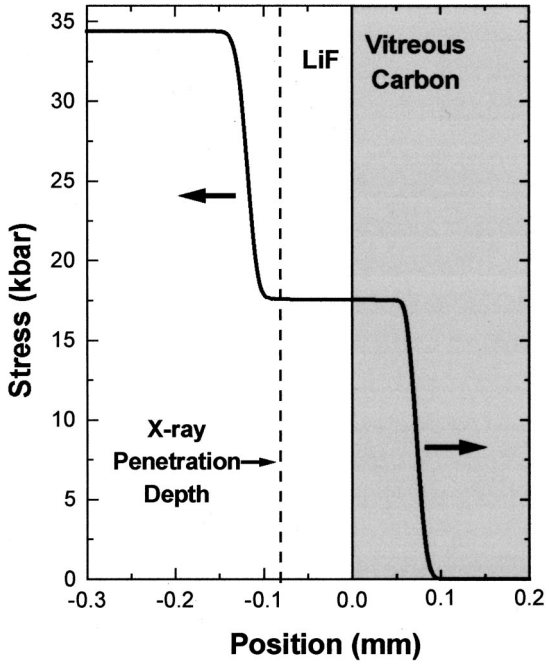

FIG. 7. Longitudinal stress-wave profile in the target at the time of x-ray exposure. The vitreous carbon back window maintains a constant stress in the probed region during the x-ray exposure time.

limit [4 GPa (Ref. 27)] for this orientation, we expected to see no lattice compression in the transverse direction.[21] Input stresses in the samples ranged from 2.7 to 3.5 GPa. The reflected stresses were lower (1.4–1.8 GPa) due to the impedance mismatch between LiF and vitreous carbon. The other four experiments were on LiF shocked along the [100] direction above the elastic limit; from the single-diffraction measurements, unit-cell compression was expected to be isotropic.[21] Input stresses in this case ranged from 2.4 to 5.1 GPa with the reflected stresses ranging from 1.6 to 3.1 GPa.

For compression along the [111] direction, the (111) diffraction peak was monitored to obtain the longitudinal lattice deformation. By monitoring changes in the (220) diffraction peak position, in conjunction with the measured longitudinal deformation, the transverse lattice deformation was determined. For compression along the [100] axis, the (200) diffraction peak was monitored to obtain the longitudinal deformation. This measurement and (202) diffraction peak shift provided the transverse deformation.

Experimental results are summarized in Table I. Projectile velocities were measured for all but one experiment using the optical technique described in Ref. 22. The input and reflected stresses and the density compression (related to macroscopic strain) at the time of the x-ray measurement were calculated using the projectile velocity and the shock data for 6061-T6 aluminum,[36,37] z-cut quartz,[38,39] LiF,[27,30] and vitreous carbon.[40] In the one case, where the projectile velocity was not obtained due to an experimental error, the projectile velocity was assumed to be 0.67 ± 0.01 mm/μs based on the mass of the projectile and the amount of powder charge used.

A. Longitudinal lattice deformation

Figures 8 and 9 show representative shifts of the (111) and (200) diffraction peaks for LiF shocked along the [111] and [100] directions, respectively; the data shown are for experiments 1 and 9. The diffraction peaks obtained on the detectors are, in general, narrow in the horizontal direction and broad in the vertical direction (see Sec. V B for representative 2D images of a diffraction peak at the CCD). However, as mentioned in Sec. III, only planar geometry is required to relate the peak shift to longitudinal changes in the unit-cell dimension; no vertical diffraction peak shift takes place in this case. The spatial shift Δx (in mm) of the diffraction peak from its ambient position is related to the change in Bragg angle, $\Delta\theta$, using

$$\Delta x = (L_0 + L_d)\tan\Delta\theta, \tag{8}$$

where L_0 is the source to target distance and L_d is the target to detector distance, and these are set equal to each other to eliminate any peak shift due to tilt.[21,32] The change in interplanar spacing is determined from Bragg's law to obtain

$$\frac{\Delta d}{d_0} = 1 - \frac{\sin\theta_0}{\sin(\theta_0 + \Delta\theta)}, \tag{9}$$

TABLE I. Summary of the multiple-diffraction plate impact experiments.

Experiment number	Projectile velocity (mm/μs)	Sample orientation	Sample thickness (mm)	Input stress (GPa)	Reflected stress (GPa)	Density compression μ (%)	Longitudinal deformation δ_l (%)	Transverse deformation δ_t (%)	Density compression μ_e (%)
1 (98-767)	0.303	[111]	0.498	2.67	1.37	0.87	0.90 ± 0.03	-0.08 ± 0.12	1.08 ± 0.54
2 (98-734)	0.307	[111]	0.499	2.70	1.39	0.90	0.87 ± 0.03	0.10 ± 0.25	0.76 ± 0.29
3 (98-714)	0.361	[111]	0.509	3.17	1.62	1.05	1.04 ± 0.04	-0.13 ± 0.18	0.80 ± 0.40
4 (98-766)	0.390	[111]	0.503	3.44	1.75	1.13	1.12 ± 0.03	-0.13 ± 0.23	0.87 ± 0.49
5 (98-738)	0.402	[111]	0.510	3.55	1.80	1.17	1.15 ± 0.04	-0.25 ± 0.26	0.66 ± 0.56
6 (98-708)	0.328	[100]	0.459	2.40	1.58	2.16	0.71 ± 0.03	0.71 ± 0.10	2.17 ± 0.24
7 (98-701)	0.483	[100]	0.483	3.58	2.29	3.09	0.95 ± 0.04	0.95 ± 0.10	2.90 ± 0.25
8 (98-755)	0.569	[100]	0.486	4.26	2.68	3.62	1.21 ± 0.04	1.18 ± 0.15	3.66 ± 0.35
9 (98-756)	a	[100]	0.536	5.06	3.13	4.18	1.36 ± 0.03	1.35 ± 0.09	4.19 ± 0.21

[a]Velocity not obtained due to experimental error.

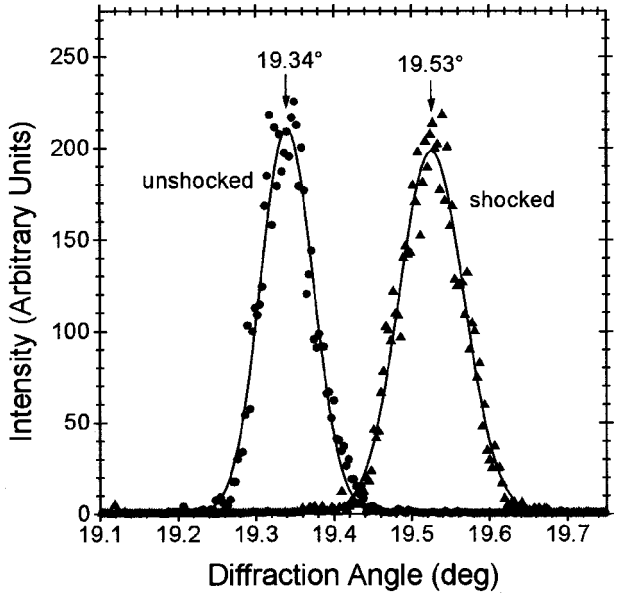

FIG. 8. Observed and fitted diffraction data from LiF showing the shift in diffraction angle due to shock compression along the [111] direction (1.4 GPa at the sample/vitreous carbon interface, experiment 1).

where d_0 and θ_0 represent the initial lattice spacing and the corresponding Bragg angle, respectively. Equations (8) and (9) were used to determine the longitudinal lattice deformation (Table I, column 8) for all of the experiments performed. The reported uncertainties arise from pulse to pulse variations in the diffraction peak position on the detector (± 1 pixel), uncertainties in measuring the peak shift, and uncertainties in measuring the source to sample and sample to detector distances (± 2 mm).

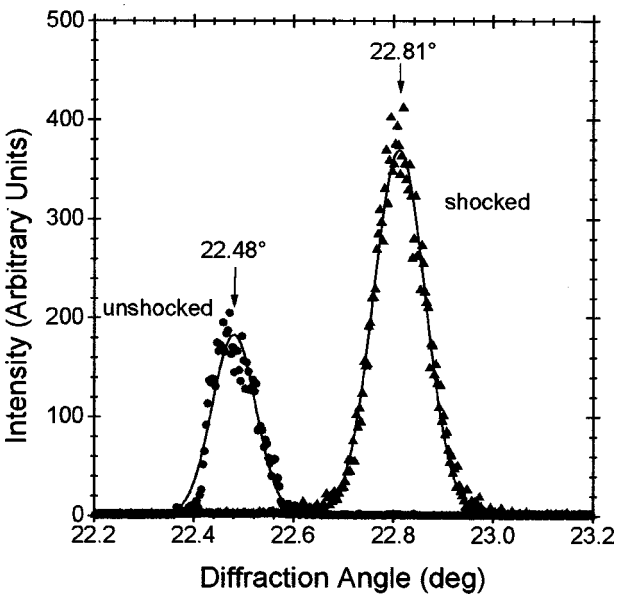

FIG. 9. Observed and fitted diffraction data from LiF showing the shift in diffraction angle due to shock compression along the [100] direction (3.1 GPa at the sample/vitreous carbon interface, experiment 9).

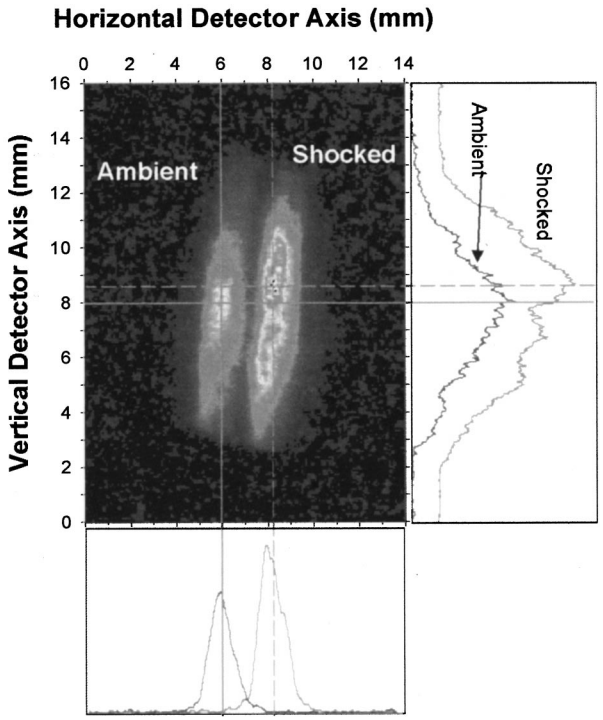

FIG. 10. CCD image showing the shifting of the (220) diffraction peak from LiF shocked along the [111] direction (experiment 1). Vertical and horizontal lineouts through the horizontal and vertical peak centers, respectively, are shown to indicate how the peak shift was determined.

B. Transverse lattice deformation

Figures 10 and 11 show the shift of the (220) diffraction peak for shock compression along the [111] and [100] directions, respectively (experiments 1 and 9). Both figures show the images of the ambient and shocked diffraction peaks, as obtained with the CCD detector. Qualitatively, the results are in good agreement with the theory showing that for compression along [111] (elastic deformation) the shift of the (220) peak is almost entirely horizontal. In contrast, for compression along [100], the (202) peak shows both a horizontal and a vertical shift as expected for isotropic compression. Also shown in the figure are vertical and horizontal lineouts through the horizontal and vertical peak centers, respectively. Quantitative results are obtained by first determining the horizontal and vertical components of the diffraction peak shift for each experiment. As seen in Figs. 10 and 11, the vertical width and profile of the diffraction peak make it difficult to accurately determine the vertical peak center. This difficulty leads to larger uncertainties in the transverse deformation measurements than in the longitudinal deformation measurements.

Due to the complexity of the diffraction geometry in this measurement, the change in lattice spacing can only be obtained directly from the peak shift if the compression is isotropic. Because isotropic compression changes the magnitude, but not the direction, of the reciprocal lattice vector for the (220) [or (202)] planes, the diffraction geometry remains two dimensional, permitting the use of the same analytical approach as used for the longitudinal measurements. For

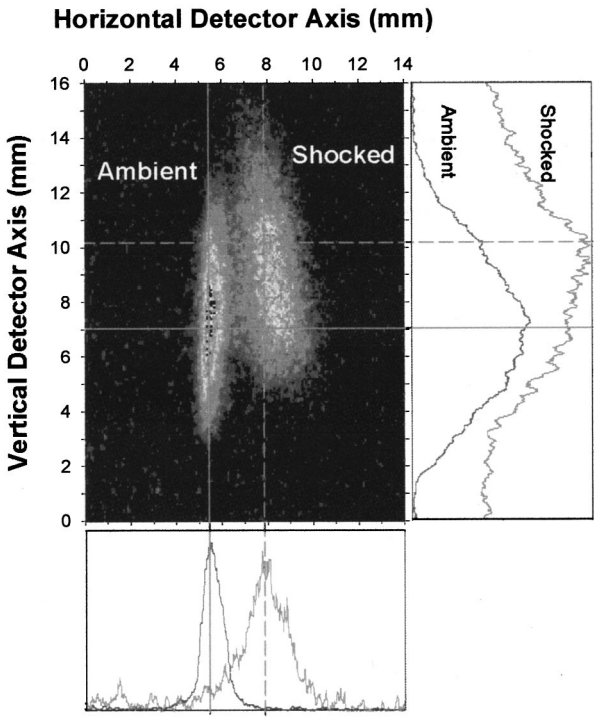

FIG. 11. CCD image showing the shifting of the (202) diffraction peak from LiF shocked along the [100] direction (experiment 9) together with the vertical and horizontal lineouts through the horizontal and vertical peak centers, respectively.

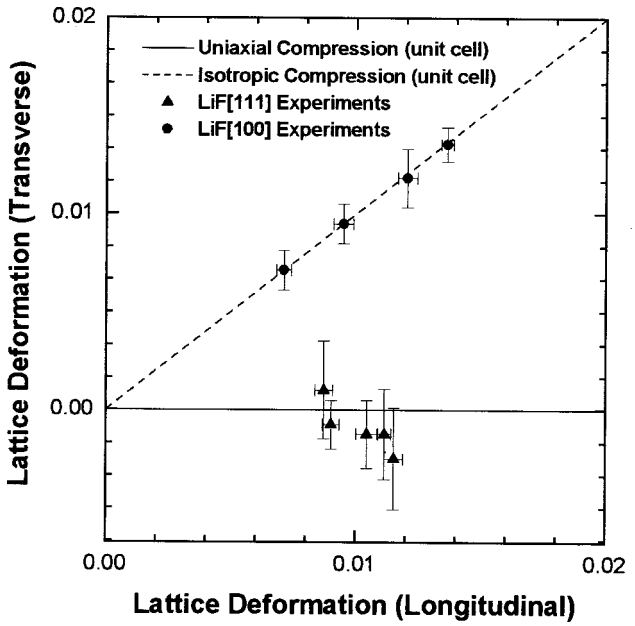

FIG. 12. Comparison of the lattice deformation in the longitudinal vs transverse directions for shock propagation along the [111] and [100] directions. The solid and dashed lines represent predictions based on uniaxial and isotropic compression of the unit cell, respectively.

nonisotropic lattice compression, the analytical model presented in Sec. III must be used to determine the transverse lattice deformation. To do this, the longitudinal deformation determined from the primary diffraction planes is entered into the calculation. Then the value of the transverse deformation is varied until the calculated shift of the diffraction peak is in reasonable agreement with the shift observed experimentally. For consistency, compression was initially considered to be nonisotropic for all experiments. The transverse deformations obtained are listed in column 9 of Table I.

Figure 12 shows the results from all experiments by plotting the longitudinal and transverse lattice deformations. Also shown in the figure are the expected results for uniaxial and isotropic compression of the unit cell. Comparison of the experimental results to the bounding cases shows conclusively that in the case of elastic deformation ([111] experiments) unit-cell compression is uniaxial, as expected. As in our previous experiments,[21] the [111] experiments serve as an important validation of our experimental and analytical method for determining the transverse deformation in shock-compressed single crystals. In contrast to the [111] experiments, compression in the [100] direction (elastic-plastic deformation) clearly leads to isotropic compression of the lattice in the shocked state at least for the ultrapure or soft LiF.

C. Density compression

Since both the longitudinal and transverse lattice deformations were measured in these experiments, it is possible to calculate directly the density compression from the experimental data. If δ_l and δ_t represent the longitudinal and transverse deformations, respectively, then the experimentally determined values of the density compression, listed in column 10 of Table I, are obtained from

$$\mu_e=[(1-\delta_l)(1-\delta_t)^2]^{-1}-1. \tag{10}$$

A comparison of the values in column 10 and the macroscopic densities obtained from the Hugoniot data,[27,30] in column 7, provides another consistency check on the developments reported here. Good agreement is seen between the calculated and measured density compression values for all of the experiments. This comparison reflects the comparison presented in Fig. 12, showing better agreement for the [100] experiments than for the [111] experiments. The latter values also have larger uncertainties. However, both sets of results demonstrate that density compression values from the existing Hugoniot data are consistent with the values obtained using the multiple-diffraction technique.

VI. SUMMARY AND CONCLUSIONS

Experimental and analytical methods were developed to determine lattice compression parallel and perpendicular to the shock propagation direction in a single crystal subjected to plane shock-wave loading. We chose to investigate LiF shocked along the [111] and [100] directions to build on our previous work.[21] With the earlier developments,[21,22] only the longitudinal lattice deformation could be measured. To obtain information about the overall compression of the unit cell, it was necessary to use bounding calculations to relate our longitudinal measurement to the macroscopic volume

compression calculated from the material Hugoniot.[27,30] As such, this approach cannot be used in general. In the present work, the unit cell compression was determined directly by using multiple diffraction to monitor lattice spacing changes simultaneously from two sets of planes. For shock propagation along the [111] and [100] directions, the planes perpendicular to the shock propagation direction [(111) and (200) planes, respectively] were always monitored to obtain the longitudinal lattice deformation. The second set of planes monitored was chosen to be the (220) planes because the relative intensity of a (220) reflection is high.

Due to the complex geometry associated with the multiple-diffraction technique, it was necessary to develop an analytical method to relate the observed diffraction peak shift from the second set of diffraction planes to the transverse lattice deformation. The present findings demonstrate directly that shock-induced elastic deformation results in uniaxial lattice compression. In contrast, shock-induced elastic-plastic deformation, at least in a very soft crystal, results in an isotropic compression of the unit cell.

The present results demonstrate that unit-cell deformation in a shock-compressed crystal can be determined directly and quantitatively using multiple-diffraction measurements. The experimental method described here overcomes the limitations in Ref. 19 by using reflection, rather than transmission, measurements to determine the transverse lattice deformation. Furthermore, the similarities between LiF and NaCl suggest that Zaretsky's conclusion,[20] that plastic deformation leads to uniaxial unit-cell compression, is incorrect. Our multiple-diffraction results agree with our previous measurements and are consistent with existing continuum data. However, we believe the benefits of this approach will be realized when it is applied toward problems where the results cannot be predicted in advance. Investigations of plastic deformation in a material with a significantly higher HEL or a material that undergoes a phase transformation[41] are a few possibilities and such investigations are currently underway.[41]

ACKNOWLEDGMENTS

Kurt Zimmerman and Dave Savage are thanked for their considerable assistance with the plate impact experiments. We acknowledge Dr. E. B. Zaretsky for discussions regarding multiple-diffraction measurements during the early part of this work. Dr. S. M. Sharma is sincerely thanked for many helpful discussions about x-ray diffraction in general. This work was supported by ONR Grant No. N000149310369, DOE Grant No. DEFG0397SF21388, and in part by ARO Equipment Grant No. DAAH049510392.

*Present address: Los Alamos National Laboratory, Los Alamos, NM 87545.

[1] Y. M. Gupta, in *Shock Compression of Condensed Matter*, edited by S. C. Schmidt, R. D. Dick, J. W. Forbes, and D. G. Tasker (North-Holland, Amsterdam, 1992), p. 15.
[2] J. M. Winey and Y. M. Gupta, J. Phys. Chem. B **101**, 10 733 (1997).
[3] Y. A. Gruzdkov and Y. M. Gupta, J. Phys. Chem. A **102**, 2322 (1998).
[4] Y. A. Gruzdkov and Y. M. Gupta, J. Phys. Chem. A **102**, 8325 (1998).
[5] X. A. Shen and Y. M. Gupta, Phys. Rev. B **48**, 2929 (1993).
[6] J. M. Boteler and Y. M. Gupta, Phys. Rev. Lett. **71**, 3497 (1993).
[7] M. D. Knudson and Y. M. Gupta, Phys. Rev. Lett. **81**, 2938 (1998).
[8] Q. Johnson, A. Mitchell, and L. Evans, Appl. Phys. Lett. **21**, 29 (1972).
[9] Q. Johnson and A. Mitchell, Phys. Rev. Lett. **29**, 1369 (1972).
[10] L. A. Egorov, E. V. Nitochkina, and Yu. K. Orekin, Pis'ma Zh. Eksp. Teor. Fiz. **16**, 8 (1972) [JETP Lett. **16**, 4 (1972)].
[11] L. V. Al'tshuler, L. A. Egorov, E. V. Nitochkina, and Yu. K. Orekin, Zh. Eksp. Teor. Fiz. **81**, 672 (1981) [Sov. Phys. JETP **54**, 359 (1981)].
[12] L. A. Egorov, A. I. Barenboim, N. G. Makeev, V. V. Mokhova, and V. G. Rumyantsev, Zh. Eksp. Teor. Fiz. **103**, 135 (1993) [JETP **76**, 73 (1993)].
[13] F. Jamet, in *High Pressure Science and Technology*, edited by B. Vodar and Ph. Marteau (Pergamon, Oxford, 1980), p. 974.
[14] F. Müller and E. Schulte, Z. Naturforsch. A **33**, 918 (1978).
[15] K. Kondo, A. Sawaoka, and S. Saito, in *High Pressure Science and Technology*, edited by K. D. Timmerhaus and M. S. Barber (Plenum, New York, 1979), p. 905.
[16] E. B. Zaretskii, G. I. Kanel, P. A. Mogelevskii, and V. E. Fortov, Dokl. Akad. Nauk (SSSR) **316–321**, 111 (1991) [Sov. Phys. Dokl. **36**, 76 (1991)].
[17] J. S. Wark, R. R. Whitlock, A. Hauer, J. E. Swain, and P. J. Solone, Phys. Rev. B **40**, 5705 (1989).
[18] J. S. Wark, D. Riley, and N. C. Woolsey, J. Appl. Phys. **68**, 4531 (1990).
[19] R. R. Whitlock and J. S. Wark, Phys. Rev. B **52**, 8 (1995).
[20] E. B. Zaretsky, in *Shock Compression of Condensed Matter—1997*, edited by S. C. Schmidt, D. P. Dandekar, and J. W. Forbes, AIP Conf. Proc. No. 429 (AIP, Woodbury, 1998), p. 883.
[21] P. A. Rigg and Y. M. Gupta, Appl. Phys. Lett. **73**, 1655 (1998).
[22] Y. M. Gupta, K. A. Zimmerman, P. A. Rigg, E. B. Zaretsky, D. M. Savage, and P. M. Bellamy, Rev. Sci. Instrum. **70**, 4008 (1999).
[23] J. R. Assay, G. R. Fowles, G. E. Duvall, M. H. Miles, and R. F. Tinder, J. Appl. Phys. **43**, 2132 (1972).
[24] Y. M. Gupta, G. E. Duvall, and G. R. Fowles, J. Appl. Phys. **46**, 532 (1975).
[25] Y. M. Gupta, Appl. Phys. Lett. **26**, 38 (1975).
[26] J. J. Dick, G. E. Duvall, and J. E. Vorthman, J. Appl. Phys. **47**, 3987 (1976).
[27] Y. M. Gupta, J. Appl. Phys. **48**, 5067 (1977).
[28] J. E. Vorthman and G. E. Duvall, J. Appl. Phys. **52**, 764 (1981).
[29] K. S. Tunison and Y. M. Gupta, Appl. Phys. Lett. **48**, 1351 (1986).
[30] W. J. Carter, High Temp.-High Press. **5**, 313 (1973).
[31] J. R. Drabble and R. E. B. Strathen, Proc. Phys. Soc. London **92**, 1090 (1967).

[32] P. A. Rigg, Ph.D. thesis, Washington State University, 1999.
[33] S.-L. Chang, *Multiple Diffraction of X-Rays in Crystals* (Springer-Verlag, Berlin, 1984), p. 8.
[34] N. W. Ashcroft and N. D. Mermin, *Solid State Physics* (Saunders College, Fort Worth, 1976), p. 101.
[35] For wave propagation along a specific direction, as is the case in the present work, a diagonal representation is valid.
[36] C. D. Lundergan and W. Herrmann, J. Appl. Phys. **34**, 2046 (1963).
[37] W. M. Isbell and D. R. Christman (unpublished).
[38] J. Wackerle, J. Appl. Phys. **33**, 922 (1962).
[39] M. D. Knudson, Ph.D. thesis, Washington State University, 1998.
[40] C. Wu and Y. M. Gupta (unpublished).
[41] T. d'Almeida and Y. M. Gupta, Phys. Rev. Lett. **85**, 330 (2000).